Inelastic behavior of steel framed structure subjected to the seismic force

Autor(en): **Kato, Ben / Akiyama, Hiroshi**

Objekttyp: **Article**

Zeitschrift: **IABSE congress report = Rapport du congrès AIPC = IVBH Kongressbericht**

Band (Jahr): **8 (1968)**

PDF erstellt am: **25.05.2024**

Persistenter Link: https://doi.org/10.5169/seals-8807

Inelastic Behavior of the Steel Framed Structure Subjected to the Seismic Force

Comportement inélastique de structures en câdres d'acier soumises à des forces sismiques

Unelastisches Verhalten des Stahlrahmentragwerkes unter Erdbebenkraft

BEN KATO   HIROSHI AKIYAMA
Associate Professor   Research Associate
The University of Tokyo
Japan

Introduction

To clear the safety of the structure against earthquake, it is necessary to know the inelastic behavior of beams, columns and entire frames until their collapse state under alternating loading as the author states. This discussion concerns to evaluation of the inelastic behavior of steel structural members.

It is known that the conventional simple plastic theory cannot predict the actual inelastic behavior of the steel structures even in monotonous loading, and it can be said that this mainly comes from the fact that the strain hardening property of the material is not taken into account in that analysis, and the effect of the applied axial load is not evaluated reasonably.

We suggest the solution for the beam-column subjected to axial compression and bending moment which makes allowance for the strain hardening and the effect of the axial compression. The load deflection diagram under alternating loading is shown to be obtained from the load deflection diagram under monotonous loading by the simple definite procedure.

Furthermore, the response analysis of the one mass vibration model of the steel structure is done using the clarified inelastic characteristics, and the difference of the response is shown to be attributed to the difference of evaluation of the effect of the strain hardening upon the structure.

Inelastic Behavior of Steel Members

Monoaxial bending only is treated here, and the effect of shear stress is ignored. Lateral buckling is also out of the matter. Breaking-off and local buckling of the section element of the member are considered to be the most effective origins of the collapse of the member and these origins can be predicted by some material tests.

General feature of the stress strain relation of steel may be expressed by the diagram as shown in Fig.(1).

As the bending deformation is obtained by integration of the

curvature along member axis, to determine the moment curvature
relation is the essential procedure.

Moment Curvature Relation--- Case I when the bending moment
is applied in monotonous way: The bending moment is to be applied
about x-x axis in Fig.(2), and the section of the member is
assumed to be symmetric about the axis perpendicular to the bend-
ing axis. Axial compression is kept in constant, and the moment
increases gradually.

Let the solid line of Fig.(3) be the strain distribution
at the arbitrary inelastic state under moment M, and the broken
line be that of after infinitecimal increase of the curvature due
to the increase of moment. Then the following relation are der-
ived from the equilibrium condition of stress.

$$dH_1 = -\frac{d\phi}{\phi} H_1 , \quad dH_1' = -\frac{d\phi}{\phi} H_1' , \quad dH_2 = -\frac{d\phi}{\phi} H_2 , \quad dH_2' = -\frac{d\phi}{\phi} H_2'$$

$$dS_e = (dH_1 B_1 + dH_2 B_2)e_1 + (dH_1' B_1' + dH_2' B_2')e_2$$
$$dI_e = (dH_1 B_1 H_1^2 + dH_2 B_2 H_2^2)e_1 + (dH_1' B_1' H_1'^2 + dH_2' B_2' H_2'^2)e_2$$
$$dO = \left\{ -(dH_1 B_1 H_1 - dH_2 B_2 H_2)e_1 - (dH_1' B_1' H_1' - dH_2' B_2' H_2')e_2 \right\} /S_e$$

where ϕ: curvature $d\phi$: increment of ϕ

ε_y : strain at yield point

ε_{st} : strain at strain hardening point

e_1 : $(E_1 - E_2)/E_1$ e_2 : $(E_2 - E_3)/E_1$

H_1 : distance from the transient neutral axis to the comp-
ression fibre where the strain is equal to ε_y.

H_2 : distance from the transient neutral axis to the tens-
ion fibre where the strain is equal to $-\varepsilon_y$.

H_1' : distance from the transient neutral axis to the comp-
ression fibre where the strain is equal to ε_{st}.

H_2' : distance from the transient neutral axis to the tens-
ion fibre where the strain is equal to $-\varepsilon_{st}$.

S_e : effective area, which means the sectional area of the
ficticious elastic bar which has the equivalent axial
rigidity to the actual bar in the specified inelastic
state.

I_e : effective moment of inertia, which means the moment
of inertia of the ficticious elastic bar which has
the equivalent flexural rigidity to the actual bar
in the specified inelastic state.

dO: movement of the transient neutral axis

B_i , B_i' : width of the section at H_i , H_i' respectively.

After the increase of the curvature $d\phi$, these quantities will
change as follows.

$$H_1 \rightarrow H_1 + dH_1 + dO , \quad H_2 \rightarrow H_2 + dH_2 - dO$$
$$H_1' \rightarrow H_1' + dH_1' + dO , \quad H_2' \rightarrow H_2' + dH_2' - dO$$
$$S_e \rightarrow S_e + dS_e , \quad I_e \rightarrow I_e + dI_e , \quad \phi \rightarrow \phi + d\phi , \quad M \rightarrow M + E_1 I_e d\phi$$

M-ϕ relation may be pursued successively using the above relaion
throughout the whole strain range. Numerical calculation is perf-
ormed easily by the aid of the electronic digital computer.

Case II when the bending moment is applied alternatingly:
It is very complicated to describe the exact M-ϕ relation under
alternating bending. So by the aid of the simplified model given
below, an outline of the relation is sought after.

1. Member section is sandwitch type as shown in Fig(4).
2. Stress strain relation of steel under alternating loading
   is as shown in Fig.(5b). To be more precise, with regard
   to the stress in definite sign the stress strain relation
   has the same configuration as that under monotonous load-
   ing as shown in Fig.(5a).

On such a model it is easily understood that the M-ϕ relation
under alternating loading is obtained as shown in Fig.(6b).
Fig.(6a) shows the M-ϕ relation under monotonous bending. Comp-
aring Fig.(6a) and Fig.(6b), it can be seen that in Fig.(6b)
with regard to the bending moment in one direction the M-ϕ rela-
tion has the same configuration as that shown in Fig.(6a).

The actual shape of section differs from that provided by
the condition 1. Hence when the bending moment is removed, the
residual stress is introduced over the section. In this paper,
however, the effect of such a residual stress is assumed to be
negligible, so the M-ϕ relation obtained above becomes applic-
able to any section.

Load Deflection Curve of Steel Members--- Deflection of the
member is readily obtained by integration of the curvature corr-
esponding to the bending moment produced by the external loads.
For the exact solution numerical integration technique is effec-
tive, but in some cases approximate solution provides facility
for engineering purposes. Especially the solution under alterna-
ting loading is uselessly troublesome. Hence for this case some
devices in approximation are needed.

When the bending stress is determined uniquely by the ext-
ernal loads, the correlation between the load deflection curve
under alternating loading and that under monotonous loading is
similar to the correlation as exists in M-ϕ relation. As is shown
in Fig.(7), the load deflection diagram under alternating loading
is readily obtained from that under monotonous loading.
With regard to a definite direction of loading, the load deflec-
tion curve in Fig.(7b) has the same configuration as that in
Fig.(7a).

But in general, geometry change of the member affects upon
the bending moment distribution. In Fig.(8) two cantilever col-
umns are shown for example. When the end load is applied alter-
natingly under constant axial load P, lateral deflection produces
secondary bending. When the end load is removed after some extent
of the inelastic deformation in one direction, deflection remains
and to remove the residual moment at the fixed end, end loads of
$-P\delta/\ell$ in the case of Fig.(8a) and $-P\delta$ in the case of Fig.(8b)
are required respectively. In such a state residual stress still
remains along the member axis as shown in Fig.(9). Here, we ass-
ume that the residual stress shown in Fig.(9) has no effect upon
the load deflection relation under further application of the
end load in the opposite direction. Based on the assumption, we
can depict the load deflection curve as shown in Fig.(10), that·
is, the load deflection curve under alternating loading is obt-
ained from that under monotonous loading in the same manner as
is shown in Fig.(7). In Fig.(7) the abscissa is the basal line
whereas in Fig.(10) the broken line which shows the tentative
unloaded state of the member is the basal line, and with regard
to the load deflection relation in one side of this line, the
curve under alternating loading has the same configuration as
that under monotonous loading. From this figure it can be seen
that the summation of the plastic deformation in one direction
until collapse does not exceed the plastic deformation capacity
under monotonous loading.

Comparison with Test Result--- Load deflection curves were
obtained using the test specimens as shown in Fig.(11).
In specimen(A) the column is subjected to axial thrust and the
transverse shear force increasing proportionally according to

the following condition.

$$P = V\cos\psi \quad, \quad Q = V\sin\psi$$

Where V is the applied load.

In specimen(B) the column is subjected to constant axial load and alternating end moment conducted through beams.

Stress strain relation of the material was obtained from the stub column test, and is shown in Fig.(12). The maximum stress was reached by occurence of the local buckling of flanges.

M-ϕ relation obtained from the procedure mentioned above is shown in Fig.(13). Load deflection curve of the specimen(A) is shown in Fig.(14), and the curve of the specimen(B) is shown in Fig.(15) in which the theoretical curve under monotonous bending is shown by the curve ABC.

Collapse of the member was assumed to occur when the stress at the point where the maximum moment grows reachs σ_B over entire section. M_B corresponds to such a stress distribution. In Fig. (14) and (15) theoretical curves after collapse are drawn on the assumption that the maximum moment of the specimen is kept to be M_B.

In these figures the test results agree with the theoretical prediction fairly well, and the effect of the strain hardening upon the inelastic behavior is very remarkable.

Response Analysis of the Framed Structure

Restoring Force Characteristics--- The cantilever column shown in Fig.(16) represents the fundamental element of the framed structure subjected to seismic force. To see the general feature of resistance of the framed structure to seismic force, a simple outline of the inelastic behavior of the cantilever column is sought after through the approximate approach.

The M-ϕ relation under the constant thrust obtained above may be approximated by two linear segments ignoring the elastic part of it. The first segment is parallel to the abscissa at M_{PC}.

At first the deflection of the member is evaluated ignoring the effect of the secondary bending caused by the geometry change. In Fig.(17) the part of the column ab is in inelastic range under the given loads P and Q, the the distribution of the curvature along the member is expressed as shown in Fig.(17b). This is reduced to the simplified model as shown in Fig.(17c) in which the curvature of the inelastic part ab is approximated by the mean value of the curvatures at the both ends of ab, then

the mean value ϕ_o may be written as follows.

$$\phi_o = \frac{\phi_{st} + \phi_f}{2} = \frac{M_f - M_{PC}}{2D_{st}} + \phi_{st} \qquad (1)$$

Where ϕ_{st}: the curvature at the starting point of the strain hardening.

D_{st}: the flexural rigidity in strain hardening range. Namely the slope of the second segment.

M_{PC}: the fully plastic moment under axial force.

M_f: the fixed end moment

The lateral deflection δ_b and the slope θ_b at point b are given as follow.

$$\delta_b = (\phi_o l_1^2)/2 \quad, \quad \theta_b = \phi_o l_1$$

Then the lateral deflection at the top of the member may be given as follows.

$$\delta = \phi_o l_1 l_2 + (\phi_o l_1^2)/2 \qquad (2)$$

Where l_1: the length of the inelastic part of the member.

l_2: the length of the elastic part of the member.

As the bending effect of the thrust P is ignored, the follwing

relation will hold for any shear force Q'.

$$Q' l_2 = M_{pc} , \qquad Q' l = Q'(l_1 + l_2) = M_f$$

These are translated as:

$$l_1/l = (\alpha - 1)/\alpha , \qquad l_2/l = 1/\alpha , \qquad \alpha = M_f/M_{pc}$$

From equation(1) and (2), introducing the expression $M_{pc} = D\phi_y$, and $\beta = \phi_{st}/\phi_y$, the lateral deflection is written as follows.

$$\delta = (\frac{\alpha-1}{2} \times \frac{D}{D_{st}} + \beta)(\frac{\alpha^2-1}{2\alpha^2}) l^2 \phi_y \qquad (3)$$

Where   D: flexural rigidity in the elastic range

As the second step, the effect of the secondary bending must be taken into account. This effect is illustrated in Fig. (18) where the curve ac shows the deflected configuration of the member. Horne*had approximated this configuration by the straight line connecting the both ends of the members as shown in Fig. (18a). Then the equivalent lateral force Q which provide the same bending moment at the fixed end is given as follows.

$$Q = (M_f - P\delta)/l = (\alpha M_{pc} - P\delta)/l \qquad (4)$$

Equation (3) and (4) give the Q-δ relation.
This approximation, however, underestimates the secondary bending and the another approximation as shown in Fig.(18b) is proposed, where the point shows the coordinate (δ, $(\alpha-1)l/2\alpha$). $(\alpha-1)l/2\alpha$ denotes the midheight of the inelastic portion, and the deflected shape of the member is approximated by the straight line also. This choice seems to be rather arbitrary, but it will be shown later that this gives the better approximation to the exact solution. In this approximation the equivalent horizontal shear force is given as follows.

$$Q = \left\{\alpha M_{pc} - (\frac{2\alpha}{\alpha+1})P\delta\right\}/l \qquad (5)$$

Comparison with the exact solution is made in Fig.(19) with regard to the Q-δ relation using the same section member as shown in Fig.(11), and the same stress strain relation as shown in Fig.(12).

In the case of no axial thrust these two methods coincide, however when the axial force becomes larger, it can be seen that the later method gives better approximation than the former one. In Fig.(20) Q-δ diagram for the same member derived from the conventional theory ignoring the strain hardening is given. Comparing these two figures, it can be seen that the effect of the strain hardening is very significant.

Besides, from Fig.(19) it can be seen that the inelastic deflection curve may be approximated by the linear relation without substantial error. Hence the fundamental feature of the restoring force characteristics of the framed structure may be suggested to be the relation as shown in Fig.(10).

Response Analysis of the 1 Mass System--- Using the restorig force characteristics given in Fig.(21) the response analysis was done . For an example, one mass viburation system as shown in Fig.(21) is chosen.

The ground motion is of N-S component of El Centro 1940, May(the peak value of acceleration is 330 gals)

Governing equation of the sytem is as follows.

$$m(\ddot{y}+\ddot{y}_o)+f(y)=0$$

Where   y: deflection   , y_o: ground motion
        f(y): restoring force characteristics

Result of the analysis is given in Fig.(22). Fig.(22a) shows the residual plastic deflection after the ground motion is faded away. Fig.(22b) shows the maximum deflection during the

earthquake and Fig.(22c) shows the summation of the plastic deflection in one direction.

The ordinate of these diagram expresses the yield force coefficient which is given as follows.

$f = F_y / mg$

Where   g: acceleration of gravity

The abscissa expresses the plastic deflection divided by the initial elastic limit deflection which corresponds to the initial elastic limit stress F_y.

In these figures, the parameter K denotes the strain hardening effect. When the strain hardening does not exist, the value is equal to the slope of the basal line ff' in Fig.(21) which denotes the effect of the secondary bending by the weight of the mass.

From these figure it can be seen that the plastic deflection is considerably affected by the strain hardening effect and especially development of the residual deflection is moderated by the strain hardening.

Conclusion

The more precise aspect of the inelastic behavior of the steel members has been pursued by the experiment and the analysis which makes allowance for the strain hardening property of steel.

The effect of the strain hardening property upon the deflection response of the steel framed structure to an earthquake was evaluated, and that was shown to be very remarkable.

Reference

* Horne M.R. , Medland I.C. : Collapse Loads of Steel Frameworkes Allowing for the Effect of Strain Hardening.
Proc. Institution of Civil Engineers 1966, May

Fig.(1) Stress Strain Relation
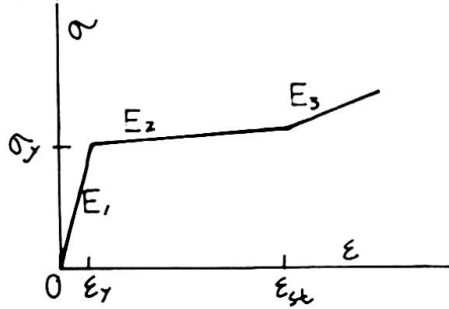
Fig.(2) Section Shape
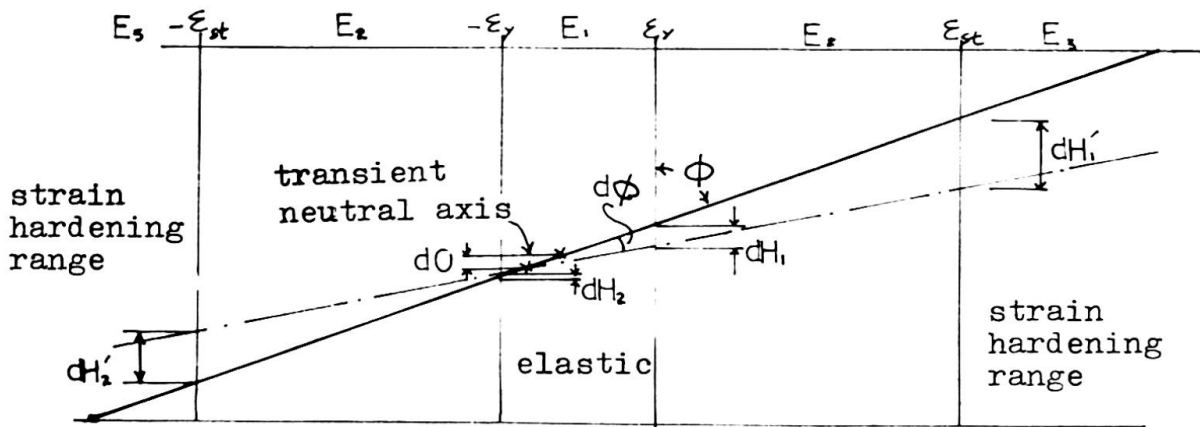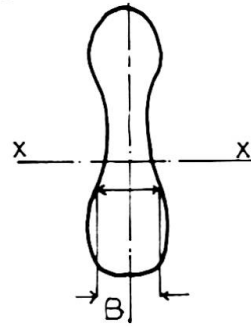
Fig.(3) Strain Distribution over the Section

Fig.(4).
Simplified
Section

(5a)
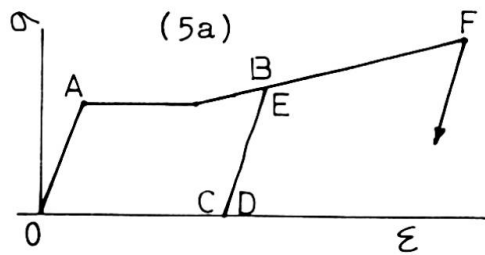
Fig.(5)
Stress Strain Relation

(5b)

(6a)

(6b)
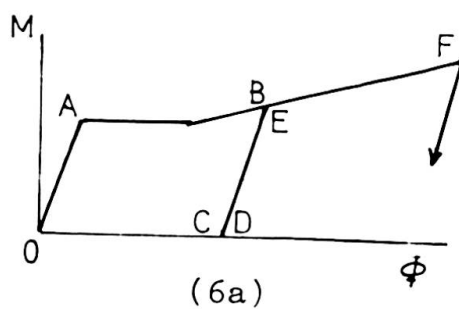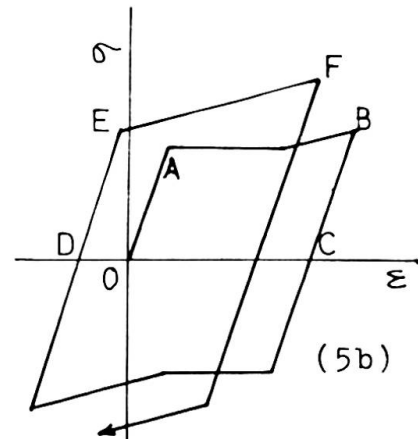
Fig.(6) M-ϕ Relation
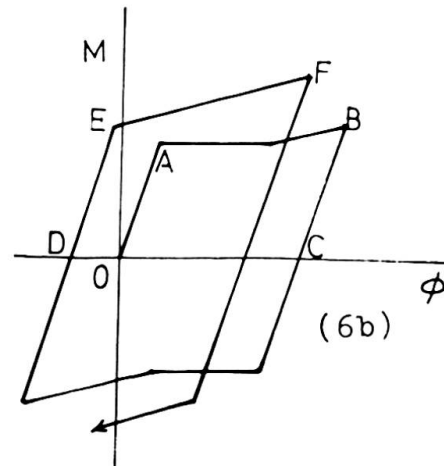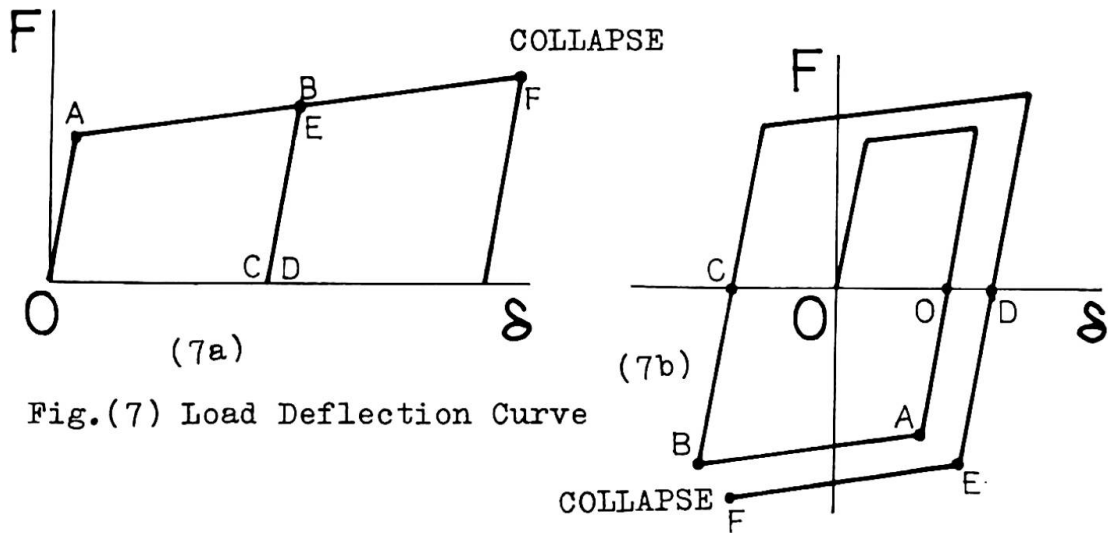
Fig.(7) Load Deflection Curve
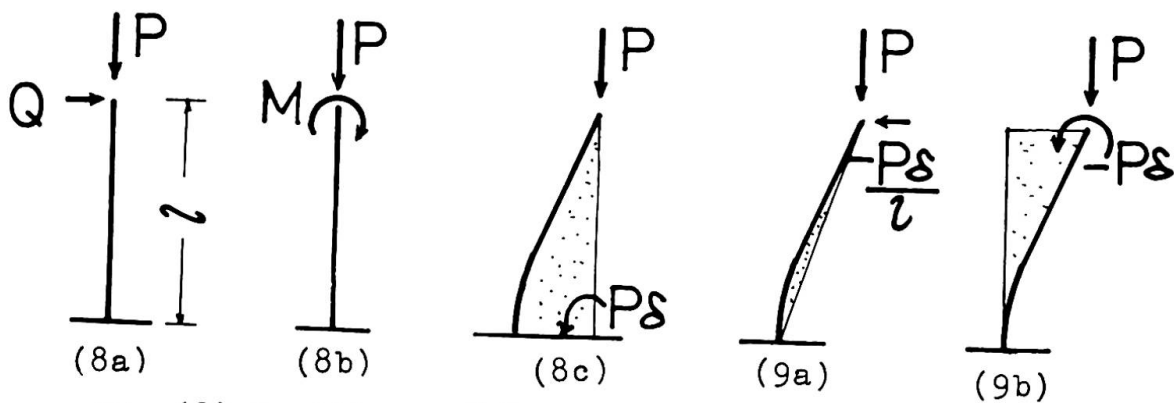
Fig.(8) Cantilever Column

Fig.(9) Residual Stress

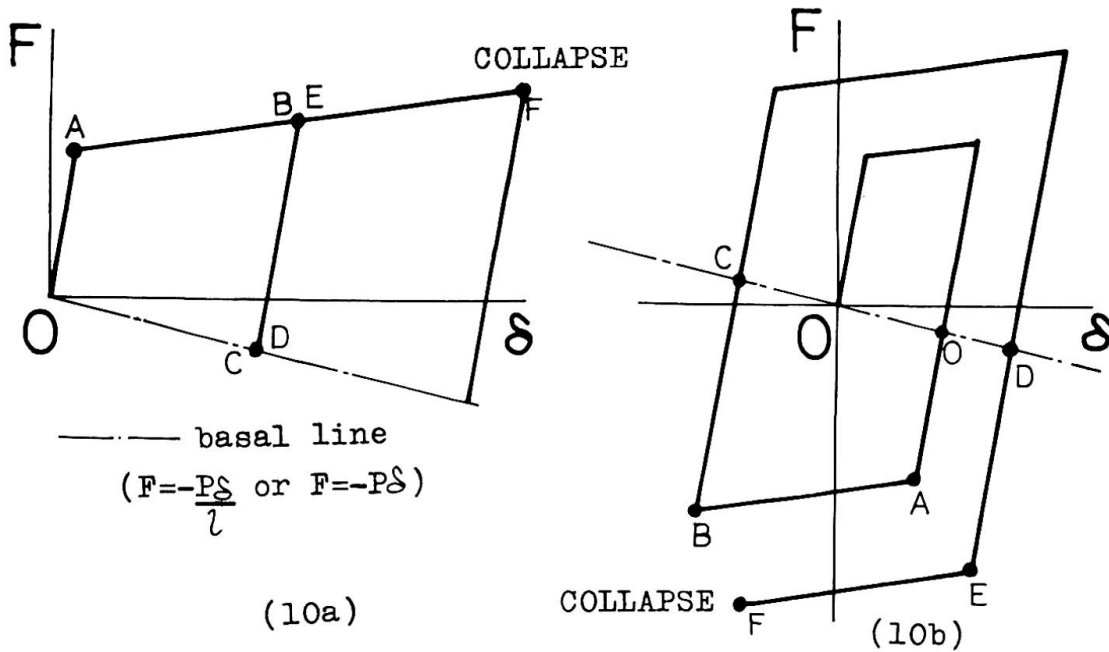
——·—— basal line

$(F=-\dfrac{P\delta}{l}$ or $F=-P\delta)$

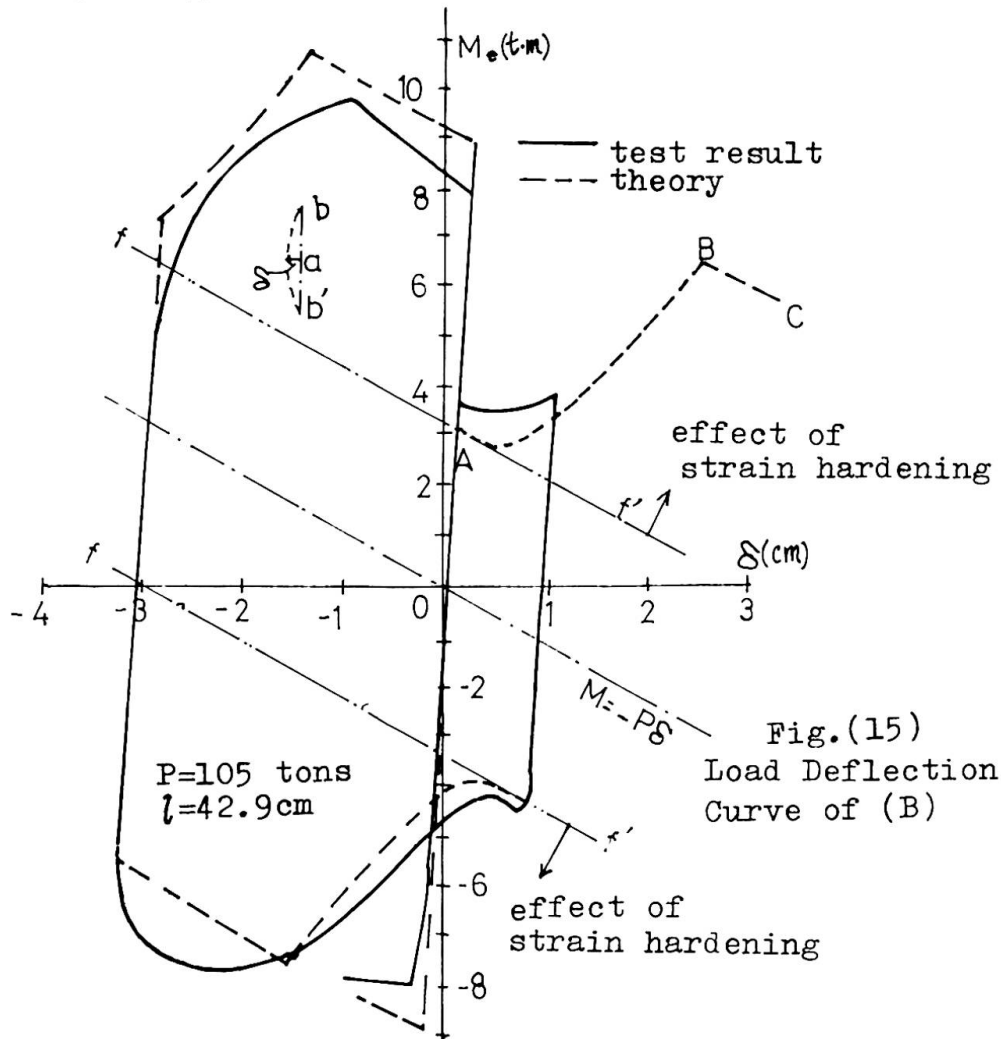Fig.(10) Load Deflection Curve under Alternating Loading

Fig.(11) Tect Specimens

(11a)
Specimen(A)

(11b)
Specimen(B)

Fig.(12)

Stress Strain
Relation

Fig.(13) The M-ϕ Relation

H : depth of section

———Fully Plastic Moment
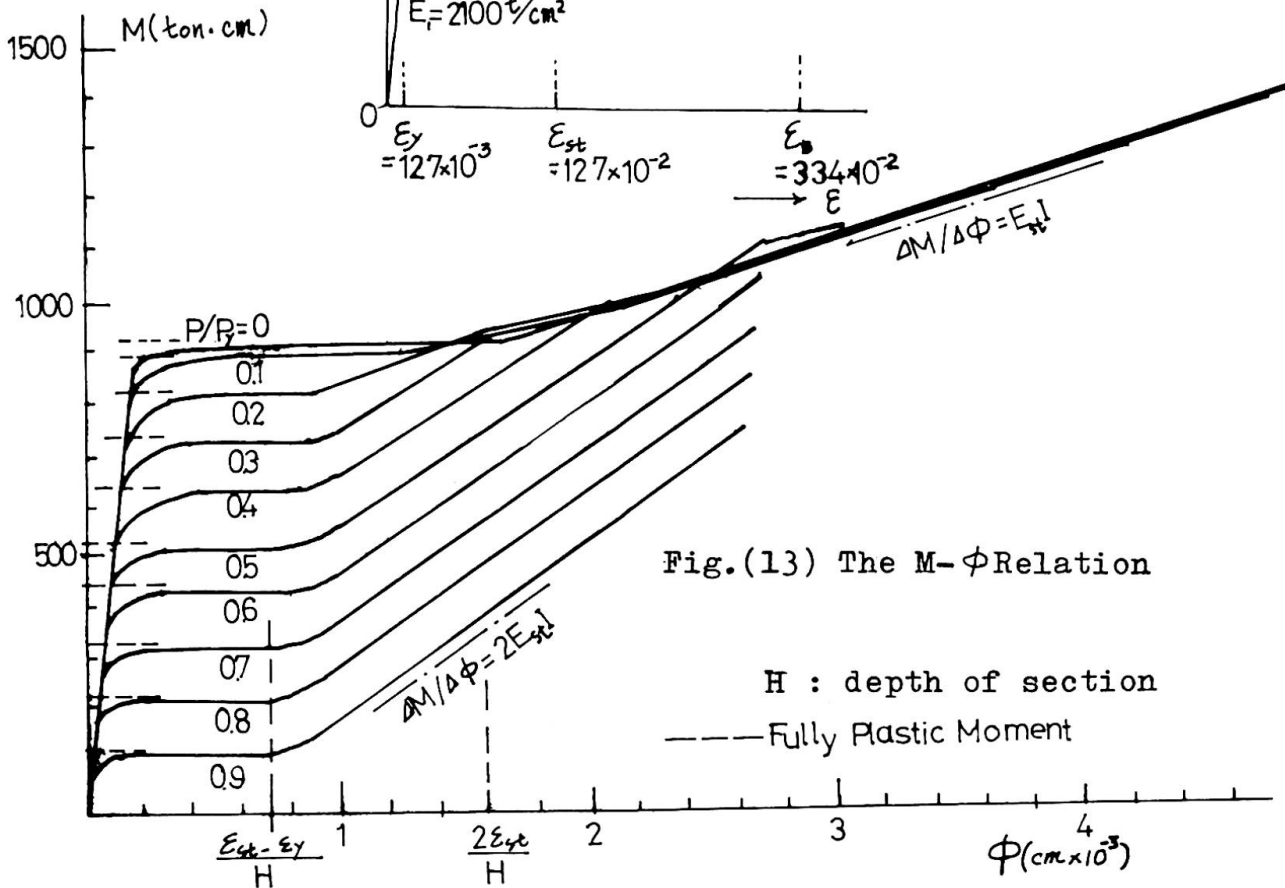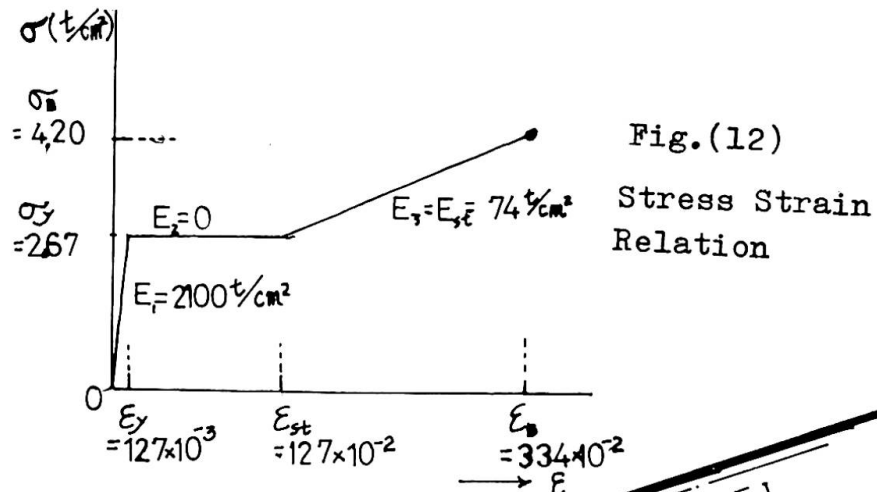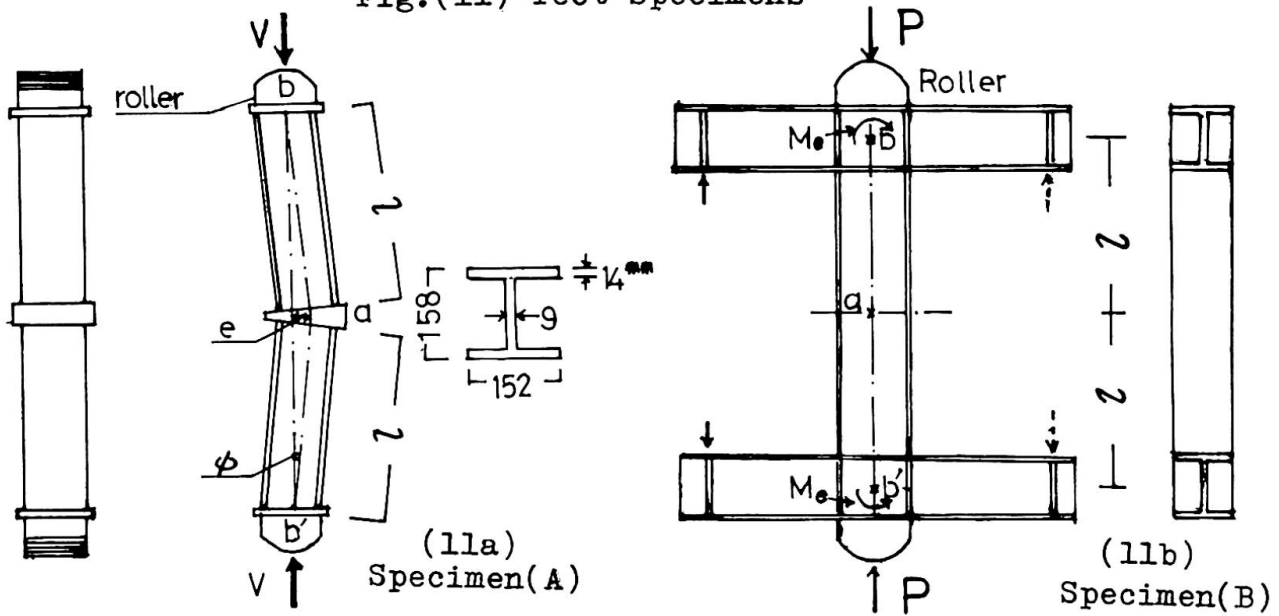
Fig.(14) Load Deflection Curve of (A)

V(ton)

—— test result
- - - exact solution
-·-·- without strain
hardening

l_{cm}	e_{cm}	V_{max}^{ton}
45	1.8	138.2

l_{cm}	e_{cm}	V_{max}^{ton}
60	6	99

l_{cm}	e_{cm}	V_{max}^{ton}
75	12.5	69.6

l_{cm}	e_{cm}	V_{max}^{ton}
90	13.5	57.2

$M_e(t\cdot m)$

—— test result
- - - theory

effect of
strain hardening

$M = -P\delta$

$P = 105$ tons
$l = 42.9$ cm

effect of
strain hardening
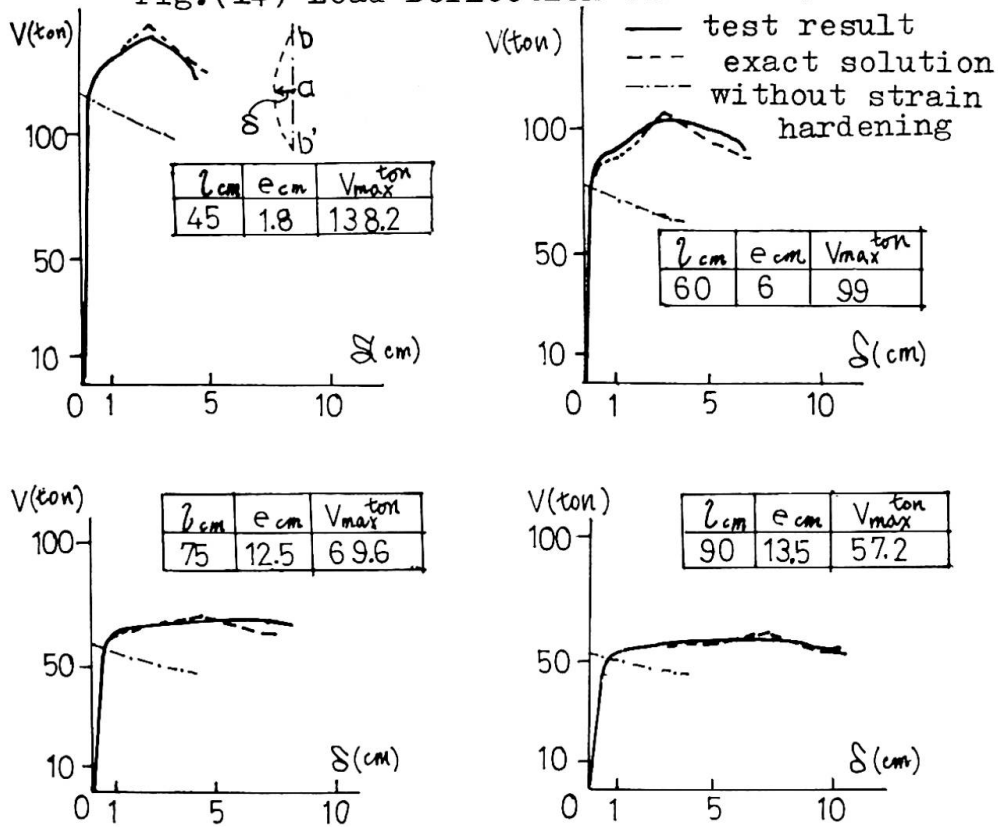
Fig.(15)
Load Deflection
Curve of (B)

Fig.(16)   Fig.(17a)

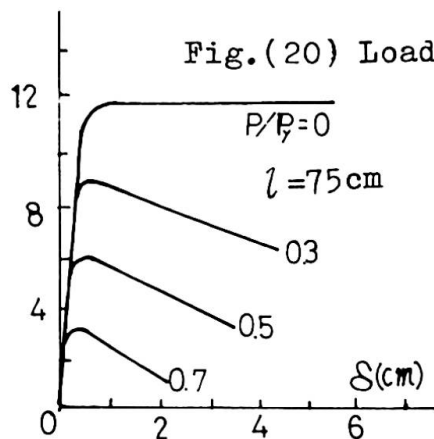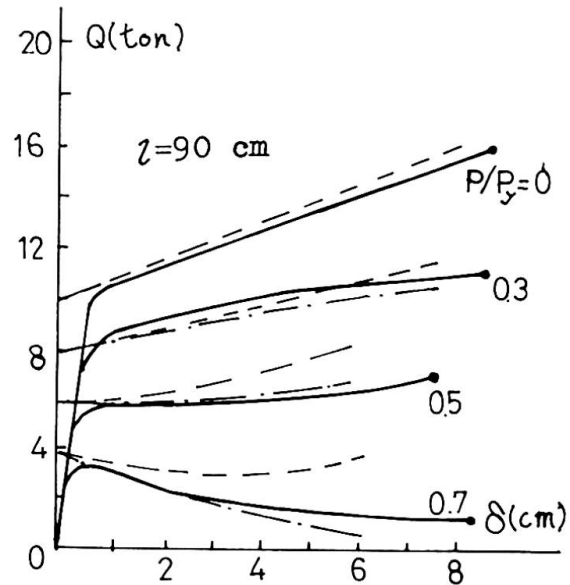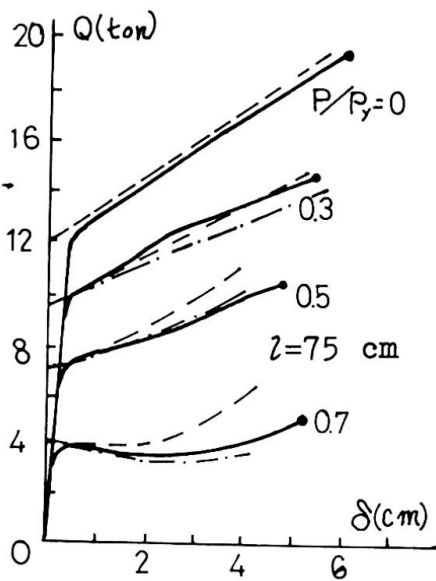Fig.(17b)   Fig.(17c)

(18a) --(I)   (18b) ---(II)
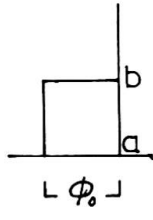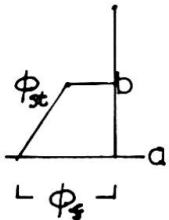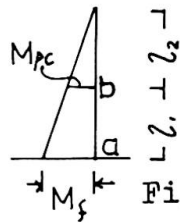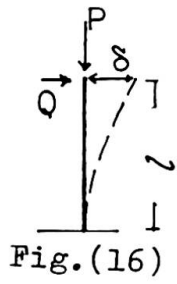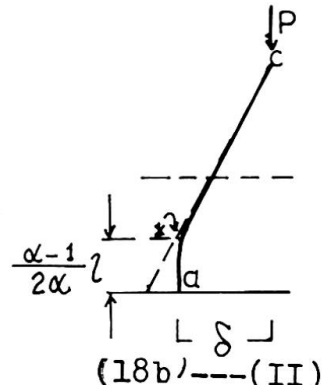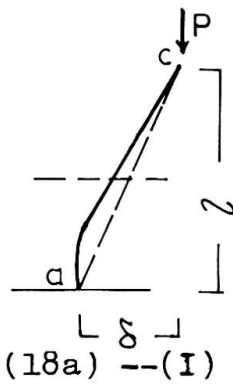
Fig.(18)   Approximated Deflection

Fig.(19) Load Deflection Curve

—— Exact Solution   • Collapse State
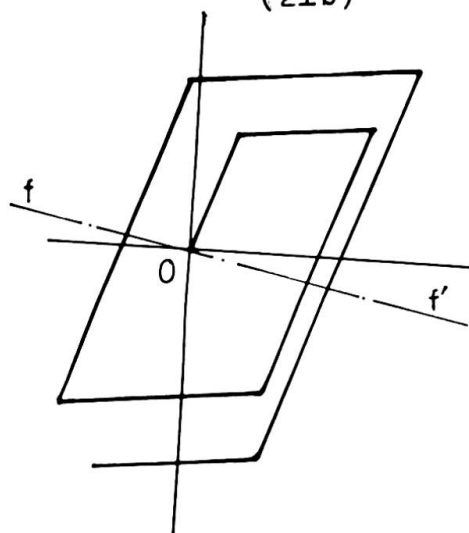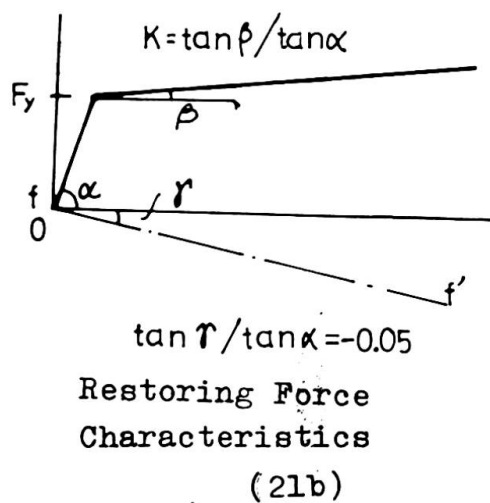
— — Approximation I   —·—·— Approximation II

Fig.(20) Load Deflection Curve P_y: yield axial force

natural period
=0.5 sec.
(21a) One Mass System

$K = \tan\beta / \tan\alpha$

$\tan\gamma / \tan\alpha = -0.05$

Restoring Force
Characteristics

(21b)

Fig.(21)

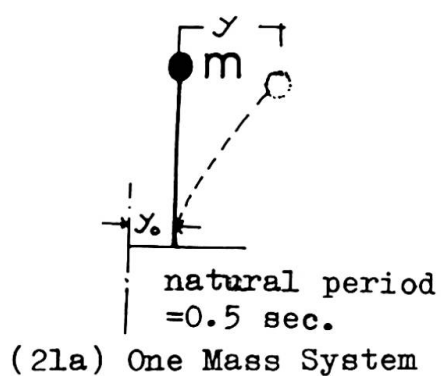$f = F_y / mg$

(22a)

$f = F_y / mg$

(22b)

$f = F_y / mg$

(22c)
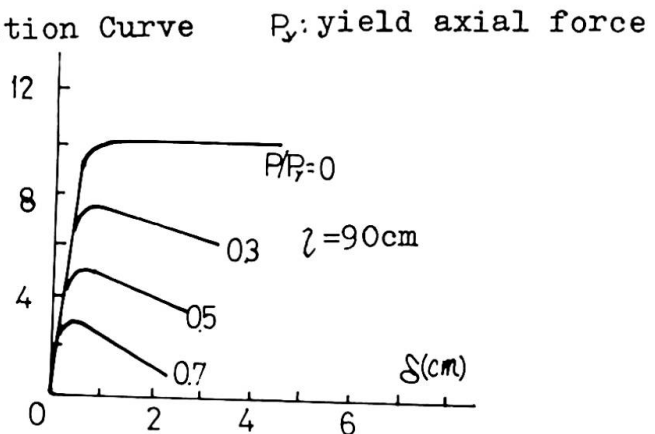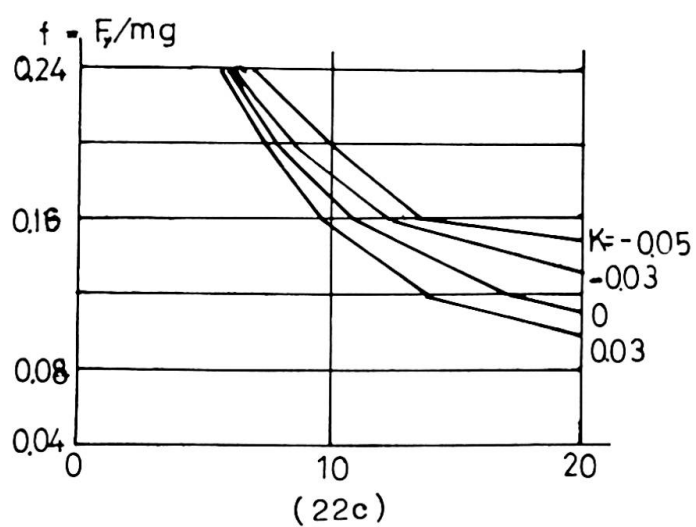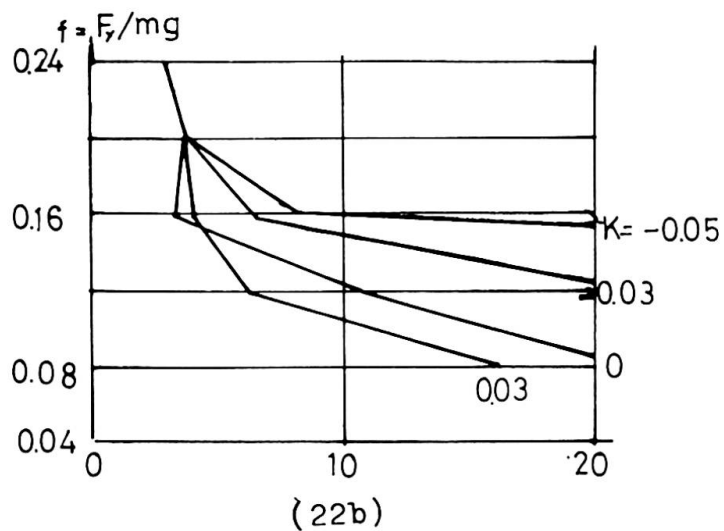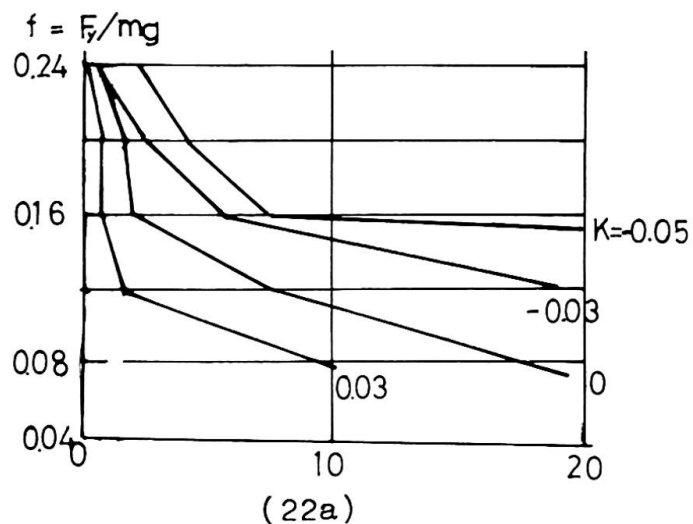
Fig.(22) Deflection Response

SUMMARY

     The more precise aspect of the inelastic behaviour of the
steel member has been pursued by the analytical method which
makes allowance for the strain hardening property of steel.

     And the effect of the strain hardening property upon the
deflection response of the steel framed structure to an earth-
quake was evaluated.

RÉSUMÉ

     Des connaissances plus précises du comportement plastique
de membres en acier ont été obtenues par la méthode analytique,
ce qui permet de tenir compte du durcissement de l'acier. Cet
effet du durcissement sur la déformation du portique d'acier due
à un tremblement de terre a été évalué.

ZUSAMMENFASSUNG

     Genaue Kenntnisse des plastischen Verhaltens von Stahlbau-
teilen wurden mit analytischen Berechnungen angestrebt, wodurch
die Verhärtung des Stahls berücksichtigt werden konnte. Die Wir-
kung der Verhärtung auf die Verformung des Stahlrahmens wurde
abgeschätzt.

Leere Seite

Blank page

Page vide